

# Simulation of Meteosat Third Generation - Lightning Imager through Tropical Rainfall Measuring Mission – Lightning Imaging Sensor data.

Daniele Biron<sup>a</sup>, Luigi De Leonibus<sup>a</sup>, Paolo Laquale<sup>b</sup>, Demetrio Labate<sup>b</sup>, Francesco Zauli<sup>a</sup>, Davide Melfi<sup>a</sup>.

<sup>a</sup>Centro Nazionale di Meteorologia e Climatologia Aeronautica, Via Pratica di Mare, 45 00040 Pomezia (RM) Italy.

<sup>b</sup>Selex Galileo, Via Einstein, 35 50013 Campi Bisenzio (FI) Italy.

## ABSTRACT

The Centro Nazionale di Meteorologia e Climatologia Aeronautica recently hosted a fellowship sponsored by Galileo Avionica, with the intent to study and perform a simulation of Meteosat Third Generation - Lightning Imager (MTG-LI) sensor behavior through Tropical Rainfall Measuring Mission - Lightning Imaging Sensor data (TRMM-LIS). For the next generation of earth observation geostationary satellite, major operating agencies are planning to insert an optical imaging mission, that continuously observes lightning pulses in the atmosphere; EUMETSAT has decided in recent years that one of the three candidate mission to be flown on MTG is LI, a Lightning Imager. MTG-LI mission has no Meteosat Second Generation heritage, but users need to evaluate the possible real time data output of the instrument to agree in inserting it on MTG payload. Authors took the expected LI design from MTG Mission Requirement Document, and reprocess real lightning dataset, acquired from space by TRMM-LIS instrument, to produce a simulated MTG-LI lightning dataset. The simulation is performed in several run, varying Minimum Detectable Energy, taking into account processing steps from event detection to final lightning information. A definition of the specific meteorological requirements is given from the potential use in meteorology of lightning final information for convection estimation and numerical cloud modeling. Study results show the range of instrument requirements relaxation which lead to minimal reduction in the final lightning information.

**Keywords:** Meteosat Third Generation, Lightning Imager, MTG LI, TRMM LIS, geostationary satellite, lightning, flash.

## 1. INTRODUCTION

The Centro Nazionale di Meteorologia e Climatologia Aeronautica recently hosted a fellowship sponsored by Galileo Avionica, with the intent to study and perform a simulation of Meteosat Third Generation - Lightning Imager (MTG-LI) [1] sensor behavior through Tropical Rainfall Measuring Mission - Lightning Imaging Sensor data (TRMM-LIS) [2].

The Lightning Imaging Sensor (LIS) is a scientific instrument that is integrated aboard the NASA, National Aeronautics and Space Administration, Tropical Rainfall Measuring Mission (TRMM) Satellite. The LIS sensor contains an optical staring imager which is used to identify lightning activity by detecting momentary changes in the brightness of the clouds as they are illuminated by lightning discharges. Due to the sensitivity and dynamic range of the sensor, it can detect lightning even in the presence of bright, sunlit clouds. The LIS instrument detects “total” lightning, since cloud-to-ground, intra-cloud, and cloud-to-cloud discharges all produce optical pulses that are visible from space [3].

For the next generation of earth observation geostationary satellite, major operating agencies are planning to insert an optical imaging mission that continuously observes lightning pulses in the atmosphere. EUMETSAT European Agency for the Exploitation of Meteorological Satellites, Darmstadt (D), considered such mission for the Meteosat Third Generation programme, with a Lightning Imager instrument.

The primary objective of the Lightning Imager (LI) is to take observations about total lightning complementary to those provided by existing and planned ground based lightning detection systems. The highest benefits will be provided in areas not covered by ground observations, particularly when located upwind of densely populated areas. The targeted detection efficiency will allow offering a consistent level of service thus providing a “space truth” reference for different ground based lightning observation systems over Europe.

MTG-LI mission has no Meteosat Second Generation heritage, but users need to evaluate the possible real time data output of the instrument to agree in inserting it on MTG payload. This study considered the LI design from Meteosat Third Generation Pre-Phase A System Architecture Study-FINAL REPORT [4]; real lightning datasets, acquired from space by NASA TRMM-LIS instrument, were processed to produce a simulated MTG-LI lightning dataset.

The simulation was performed in several runs, varying Minimum Detectable Energy and taking into account all steps: from event detection to final flashes information. Study results showed the impacts on the flash detection capability of the instruments according to various relaxations of the instrument requirements, pointing out the optimum relaxation respect to minimal reduction in flash detection performance.

## 2. LIGHTNING IMAGER INSTRUMENT

### 2.1 Lightning Imager Instrument Requirements.

Lightning Imager is expected as a unparalleled tool to monitor lightning activity in the atmosphere, already guarded from the ground by means of radiofrequency observing network, that have the limit to cover only the territory where are installed. Ground networks observe strokes, each single transfer of electric charge, especially from cloud to ground (CG) respect cloud to cloud (CC), that belong to flashes, the convolution phenomena. From flashes presence it is possible to individuate zones of stormy weather, with dense presence of convection, probable heavy rain and hail, gusty wind and turbulence. Fundamental requirement of Lightning Imager is to observe flashes, of all type, both CG and CC, to monitor storms and related phenomena over the full disk. The LI system requirement present in the Meteosat Third Generation Pre-Phase A System Architecture Study-FINAL REPORT is:

Table. 1. MTG-LI instrument features in case of one and four optical heads concept.

MTG-LI	1 Optical Head	4 Optical Heads (each)
FOV	16°	8°
Spatial resolution @ 45° N	10 km	10 km
Array Format	1414 x 1414	707 x 707
Array Size	71 mm	36 mm
Optical Diameter	300 mm	200 mm
f/number	0.84	1.3
Detection Efficiency	> 90% for 4.0 $\mu\text{Jm}^{-2}\text{sr}^{-1}$	
False Alarm Rate	< 1s <sup>-1</sup>	
Flash Temporal Signature	0.5 ms	
Filter	777.4 nm (band pass 1.4 nm)	

At the beginning of the study a mathematical model was established to evaluate instrument performance in terms of detection efficiency for a certain flash energy, given the instrument parameters and the desired false alarm rate. Adopting this model some alternative instrument solutions can be evaluated in order to best match scientific return and instrument resources allocation.

Following the huge detector size requested in case one optical head is adopted (no so large space detector having ever been realized), first solution is discarded and four optical heads concept is retained as baseline. According to the present optical layout of the lightning imager, a narrow band (1.4 nm) filter is needed by each optical head to reject most background during daylight operations, observing at 777.4 nm, OI emission line. Given the large aperture needed to fully meet the most challenging requirement (Detection Efficiency > 90% for  $4.0 \mu\text{Jm}^{-2}\text{sr}^{-1}$  energy flash), alternative solutions have been investigated, to verify if a relaxation of requirements could lead to better trade off between scientific performances and resources allocation. In particular three options has been traded, similar to the one in Meteosat Third Generation Pre-Phase A System Architecture Study-FINAL REPORT [4], based on the following drivers:

Option 1: baseline configuration described above.

Option 2: gives a lower, but still usable, detection efficiency (close to 50% chosen) for  $4.0 \mu\text{Jm}^{-2}\text{sr}^{-1}$  flash energy.

Option 2.1: optimized for 90% detection efficiency on a  $8.3 \mu\text{Jm}^{-2}\text{sr}^{-1}$  flash energy.

## 2.2 MTG-LI Overview.

Optical design for each head is specified and illustrated in Figure 1 (narrow band filter is not represented). A very simple solution in terms of number and feasibility of optical elements, fully compliant with radiation requirements of the space environment is presented. A catoptrics layout is selected with four lenses, having only one aspheric surface (first surface of the first element). Selected material is fused silica for all the lenses but the second one, that is manufactured in ZnS.

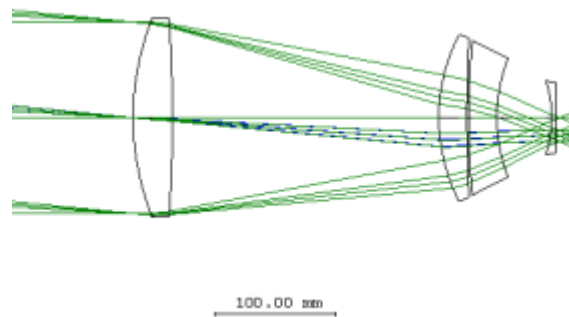


Fig. 1. Optics layout for each optical head.

A baffle is placed in front of each telescope, with acceptance angle (half aperture) of  $20^\circ$  to provide effective rejection of straylight from any source that is  $20^\circ$  or more apart from the line of sight.

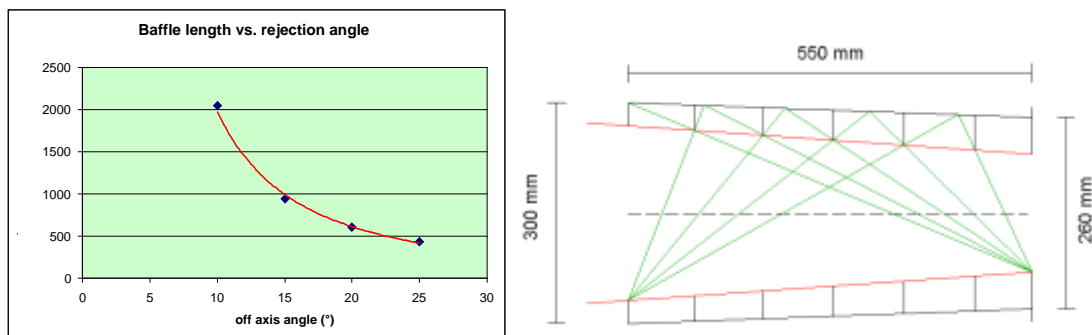


Fig. 2. LI Baffle sizing and design.

Baseline detector technology is a hybrid CMOS detector. This allows the highest efficiency, together with the possibility to implement some processing functions at a pixel level. In fact, since frame rate is very high, but useful lightning information contained in each frame is as low as few pixels, a readout approach is proposed in which frames are not fully transferred to the proximity electronics. Instead, appropriate detector read-out integrated circuit design and operation allows extraction of flash information at detector level (by evaluation of background and thresholding), with a dramatic reduction of the throughput. In this way, complexity of the proximity electronics and associated resources (mainly power) are significantly reduced.

Detector specification are reported in Table 2, second column, together with a layout of the integrated pixel level pre-processing electronics. Integration time of 0.8 ms is adopted in order to optimize coupling between frame rate and flash temporal signature. Read while integrate mode is selected to avoid any dead time between frames. Readout of only those pixels that exceed threshold is achieved thanks to the detector architecture, according to the following steps:

1. fast scan of the row events until one is found to be high,
2. pixel events and pixel outputs (of the relevant row) transfer to the output register,
3. row scan through sequential column addressing,
4. ADC conversion only of those pixels whose event flag is found to be high,

Table. 2. CMOS detector specification.

Parameter	CMOS Value	APS Value
Quantum efficiency x fill factor	80 %	70 %
Well capacity to meet dynamics	$2 \times 10^6$ e-	$1.5 \times 10^6$ e-
Readout + fixed noise	350 e-	400 e-
Array format	778 x 778 pixels	778 x 778 pixels
Pixel pitch	40 $\mu$ m	40 $\mu$ m
Operation	snapshot	snapshot
Frame rate	1250 fps	1250 fps
Pixel detection	CTIA	CTIA
Max handling capacity	50 events/frame	50 events/frame
ADC	12 bit	12 bit

Note that, due to the relatively low maturity criticality of the hybrid CMOS technology in Europe, a backup solution is presented, too. It is constituted by a backside illuminated monolithic active pixel sensor (APS), that still shows a good quantum efficiency times fill factor product (even if not at the high level of a monolithic APS) and whose development efforts and time appears to be smaller, according to the European manufacturer contacted. Specification of the backup focal plane array is contained in Table 2, third column. Same pixel level electronics and readout architecture illustrated above are foreseen even for this backup option. Resulting instrument layout is constituted by a bench structure supporting the four optical heads, proximity electronics boxes (one per head) and a radiator. It is illustrated in Figure 3.

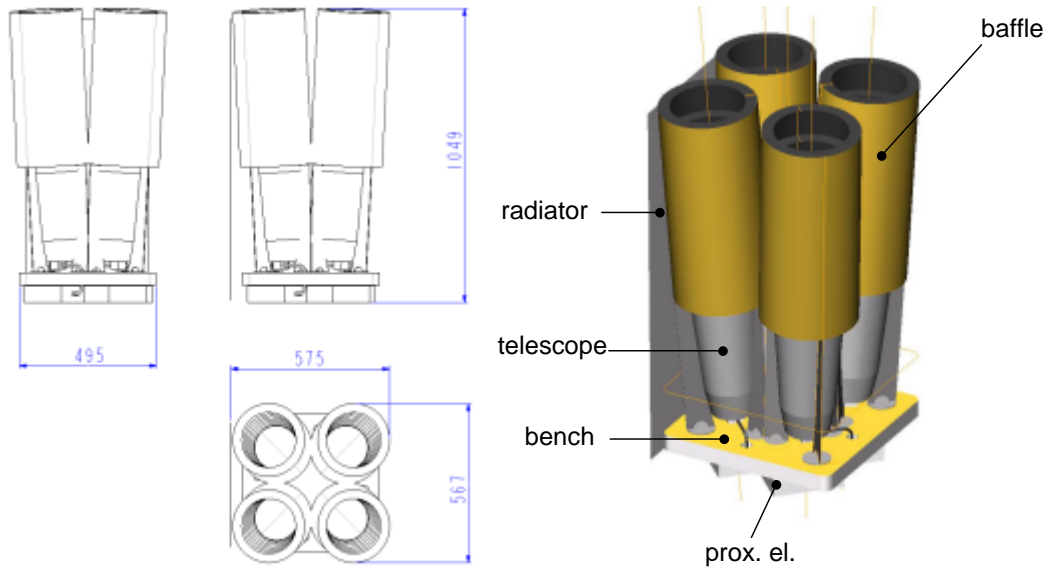


Fig. 3. MTG - Lightning Imager layout, sizing in mm.

Instrument performance, for several effective optics diameter and quantum efficiency compatible with the four heads configuration, are summarized in figure 4,5,6 and 7, where detection efficiency is plotted versus flash energy, for different values of false alarm rate (number of false detections over the whole covered FOV). Worst case for flash detection (i.e. maximum background during day) is considered in all cases.

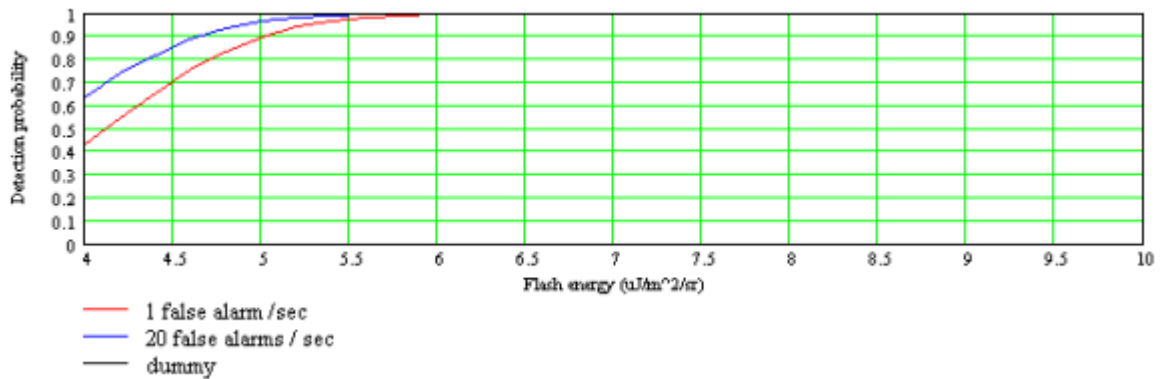


Fig. 4. Effective Optics Diameter = 160 mm; QE = 80%.

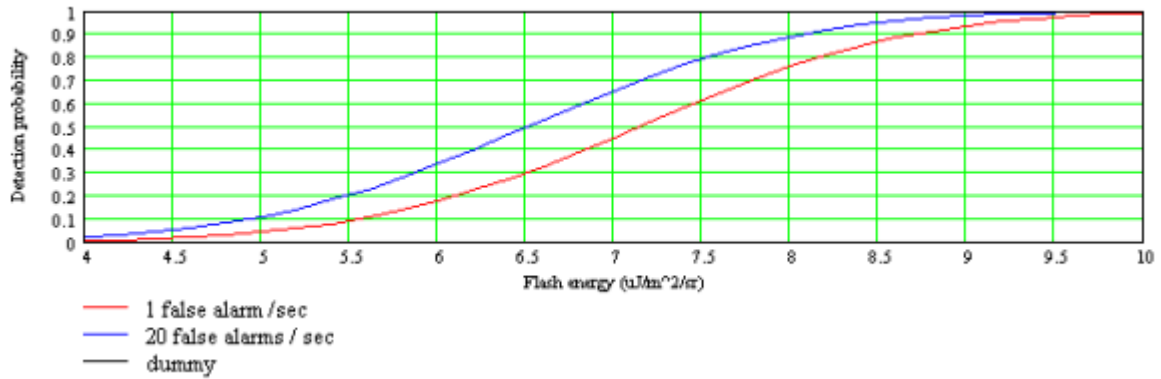


Fig. 5. Effective Optics Diameter = 100 mm; QE = 80%.

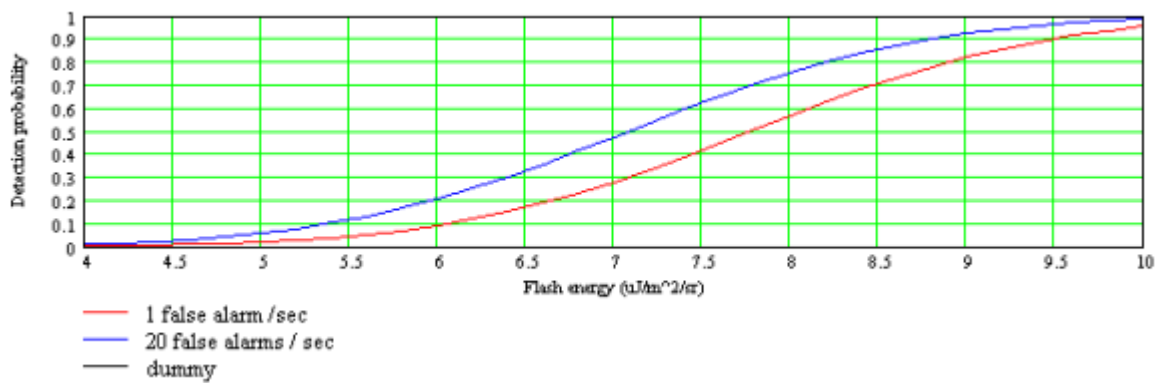


Fig. 6. Effective Optics Diameter = 100 mm; QE = 70%.

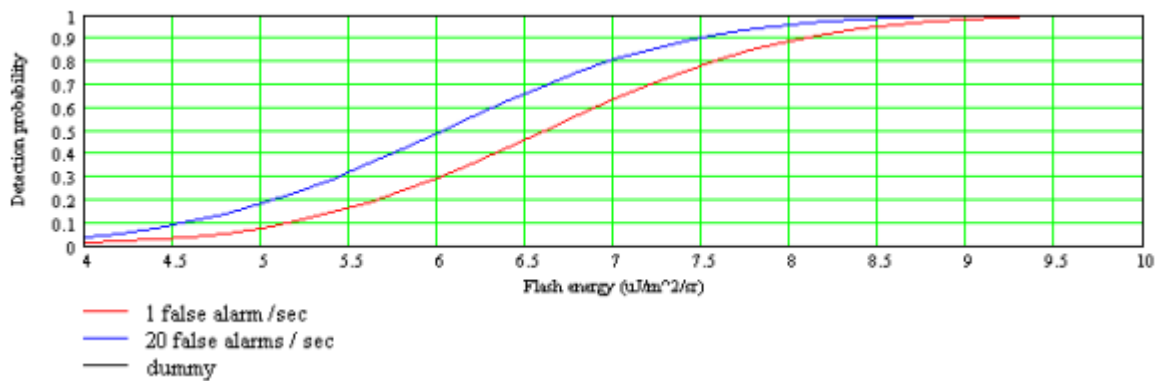


Fig. 7. Effective Optics Diameter = 110 mm; QE = 75%.

One of the best results obtained for the relaxation of the requirements is showed in figure 7. In this case, the instrument design is optimized for 90% detection efficiency at  $8.3 \mu\text{Jm}^{-2}\text{sr}^{-1}$  flash energy. The goal of the MTG-LI simulation, presented in the next section, is to estimate the impact on flash detection capability of the instruments requirements relaxation, from initial instrument requirements presented in Table 1 towards the ones belonging to the proposed Option 2.1 of Meteosat Third Generation Pre-Phase A System Architecture Study-FINAL REPORT [4].

### 3. THE SIMULATION

#### 3.1 Simulation steps.

MTG-LI mission has no Meteosat Second Generation heritage, but users need to evaluate the possible real time data output of the instrument to agree in inserting it on MTG payload. This study considered the MTG-LI design from Meteosat Third Generation Pre-Phase A System Architecture Study-FINAL REPORT, LI instrument configuration as reported in Option 2.1 [4]; real lightning datasets, acquired from space by NASA TRMM-LIS instrument [5], were processed to produce a simulated MTG-LI lightning dataset. It was decided to use for the simulation only LIS instrument data of the NASA Tropical Rainfall Measuring Mission, launched in low earth orbit, over tropical latitudes (Figure 8), during November 1997, because they are freely available at NASA web site, for all the lifetime of TRMM, in files containing every data, till the lowest and more detailed level of information, already calibrated, geo-located, with error filtrated out. The Optical Transient Detector (OTD) data, the previous optical lightning detector managed by NASA, payload of Orbview-1 satellite launched in low earth near polar orbit, during April 1995, were not suitable to the purpose because they are not available at detailed level of information easily.

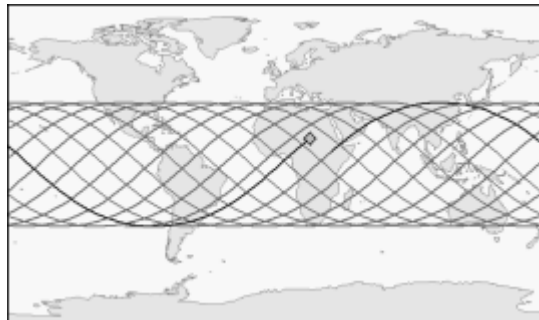


Fig. 8. The LIS field-of-view and the orbital track of the TRMM satellite during a 24 hour period (NASA).

NASA-LISAPP software was used and modified for processing the mentioned LIS data to simulate the events, groups and flashes as could be observed by MTG-LI. For the simulation were selected LIS data along the year 1998, the first year of the satellite operations, in which it could be expected the best performance of the instrument during lifetime. We took into consideration 10 pass of the satellite for every month of all the year over the equatorial zone from  $-15^\circ$  west longitude to  $15^\circ$  east longitude, and from  $-15^\circ$  south latitude to  $15^\circ$  north latitude, equally distributed in day, night and twilight cases. In this way we are sure that the population of events detected from space is statistically significant, as clear from lightning distribution as observed from OTD sensor in Figure 9.

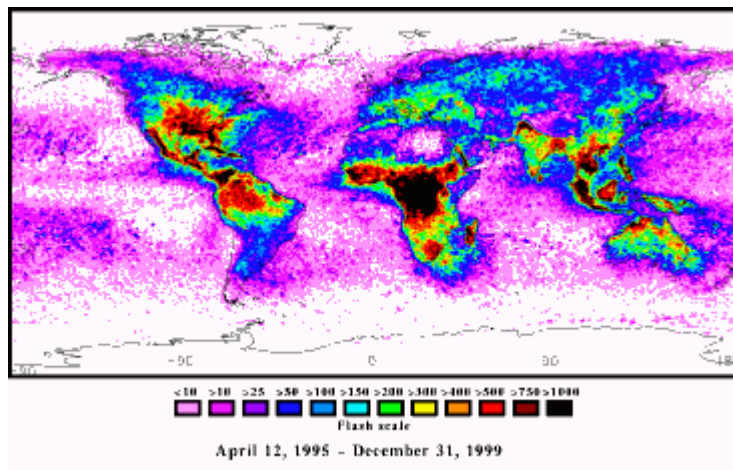


Fig. 9. The lightning distribution, as observed by OTD sensor (NASA).

Simulation was performed to obtain observed events according to the three constraints regarding Minimum Detectable Energy and Detection Efficiency:

1. without restriction in radiance as Option 1 initial concept (minimum detectable energy  $4.0 \mu\text{Jm}^{-2}\text{sr}^{-1}$ ).
2. with restriction to radiance greater than  $8 \mu\text{Jm}^{-2}\text{sr}^{-1}$ , as in Option 2.1.
3. with restriction to radiance greater than  $10 \mu\text{Jm}^{-2}\text{sr}^{-1}$ , a limit that, as clear from Figure 4 to 7, represents a threshold with no impact on instrument design, so that it can reach best performance with small optics.

For all these three general constraints we performed the following steps: loading of TRMM-LIS data granules, storing only quality controlled events, filtering out events with calibrated radiance under the threshold considered and out of the analyzed scene, resample remained TRMM-LIS events in MTG-LI events in consideration on the position of the satellite and the pixel dimensions, grouping by weighing same timestamp and near LIS events, within LI pixel dimensions, to build LI events position, timestamp and radiance.

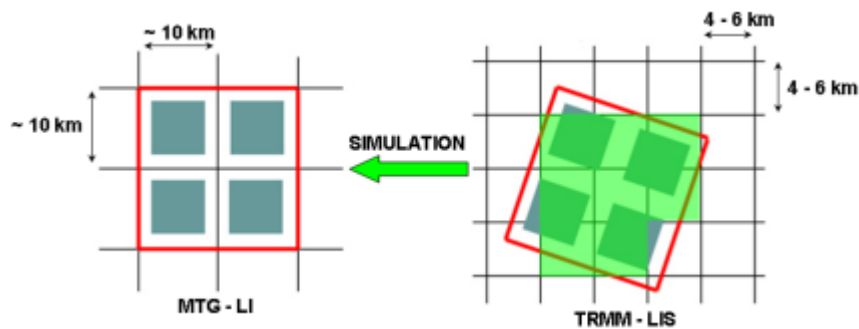


Fig. 10. The filtering and resample of TRMM-LIS event dataset to built MTG-LI event population.

The data aggregating technique is the same to the one applied by NASA in the treatment of LIS event dataset. The accumulation types in NASA technique are four: 1) events, 2) groups, 3) flashes, 4) areas. The first level of information present in LIS dataset is the one of events, the report of each single switch on of pixels (incoming radiance beyond threshold) in the acquiring matrix of the instrument. In LIS data granules we downloaded, NASA has already removed artefacts such as duplicated data point, ghosts, lollypops, blasts, cosmic ray particle tracks and any other false alarms. So we could process directly all LIS events as real, producing, after radiance threshold based filtering, resample, grouping and weighing, MTG-LI simulated events.

If events are contiguous in LI matrix position and with same timestamp they are accumulated in one group, for example in first step of Figure 11 at generic time  $T_0$  events 1,2 and 3 occur contiguously and in the same time, they are aggregated in group a. In this example (Figure 12) events are indicated with numbers, groups with lower case letters, flashes with upper case letter and areas with greek letter. At subsequent time  $T_1$  (within 330 ms from  $T_0$ ) events 4 and 5 occur, they are contiguous and having the same time and are accumulated in group b, group b is contiguous to groups a, then they are aggregated in flash A. At subsequent time  $T_2$  (being less than 330 ms the  $T_2-T_1$  time gap) events 6, 7 and 8 occur, they are accumulated in group c, contiguous to group b, than associated to same flash A.

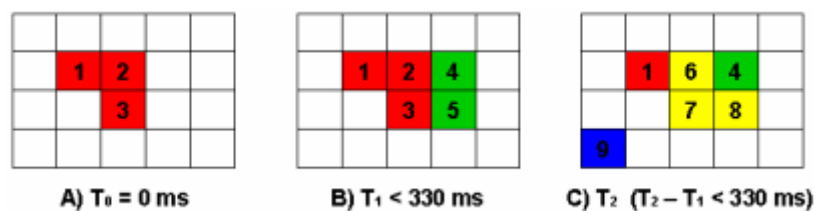


Fig. 11. Events, groups, flashes, and areas accumulating technique: the matrix.

At the same time event 9 occur, it is not contiguous to any other events, so it constitutes group d, that is not contiguous to any other groups in a time slot of 330 ms, so it produces new flash B. Being closer than 16.5 km and with time gap less than 330 ms, NASA accumulate flash A and B in area , condensing further lightning information. We do not perform this type of accumulation because to much brief, preferring to discuss final computed lightning information at flash level.

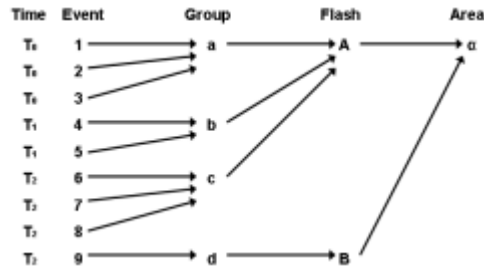


Fig. 12. Events, groups, flashes, and areas: example accumulation diagram.

Obtained simulated data were sorted according to: date, hour, distinction in day, night and twilight, events, groups and flashes without restriction in event radiance; events, groups and flashes with restriction to event radiance greater than  $8 \mu\text{Jm}^{-2}\text{sr}^{-1}$ ; events, groups and flashes with restriction to event radiance greater than  $10 \mu\text{Jm}^{-2}\text{sr}^{-1}$ .

### 3.2 Statistics on simulated populations.

The population of events, groups and flashes surviving to the mentioned radiance restrictions were computed (greater than  $8 \mu\text{Jm}^{-2}\text{sr}^{-1}$  and greater than  $10 \mu\text{Jm}^{-2}\text{sr}^{-1}$ ) and they were compared with the events, groups and flashes computed without restriction in radiance. Statistics of the surviving fraction were computed along all year 1998 and are reported in Table 4 and in the Figures 13 – 18.

Table. 4. Statistics of the surviving fraction of events, groups and flashes.

Survival Percentage	Events $8\mu\text{Jm}^{-2}\text{sr}^{-1}$	Events $10\mu\text{Jm}^{-2}\text{sr}^{-1}$	Groups $8\mu\text{Jm}^{-2}\text{sr}^{-1}$	Groups $10\mu\text{Jm}^{-2}\text{sr}^{-1}$	Flashes $8\mu\text{Jm}^{-2}\text{sr}^{-1}$	Flashes $10\mu\text{Jm}^{-2}\text{sr}^{-1}$
Mean	43,3	32,5	56,0	45,0	85,6	78,6
Std. Dev.	13,4	12,4	11,4	11,8	9,4	12,0

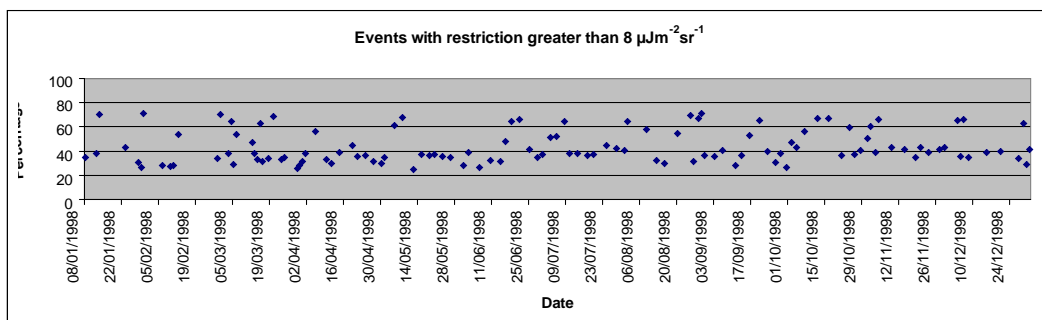


Fig. 13. Comparison between events greater than  $8 \mu\text{Jm}^{-2}\text{sr}^{-1}$  and events without restriction in radiance

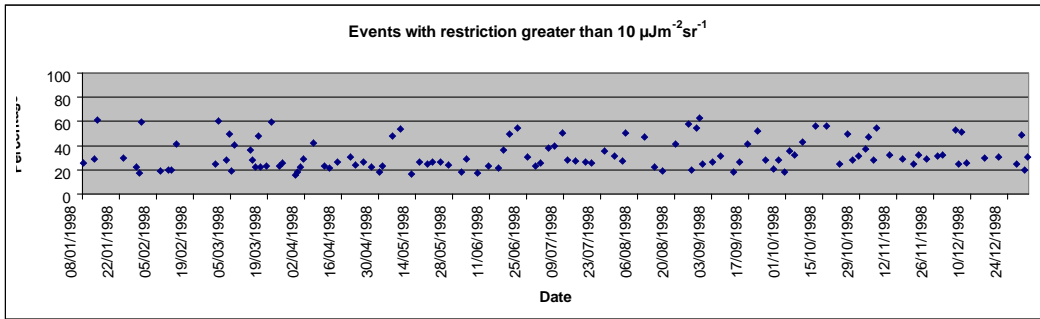


Fig. 14. Comparison between events greater than  $10 \mu\text{Jm}^{-2}\text{sr}^{-1}$  and events without restriction in radiance



Fig. 15. Comparison between groups derived from events greater than  $8 \mu\text{Jm}^{-2}\text{sr}^{-1}$  and groups derived from events without restriction in radiance

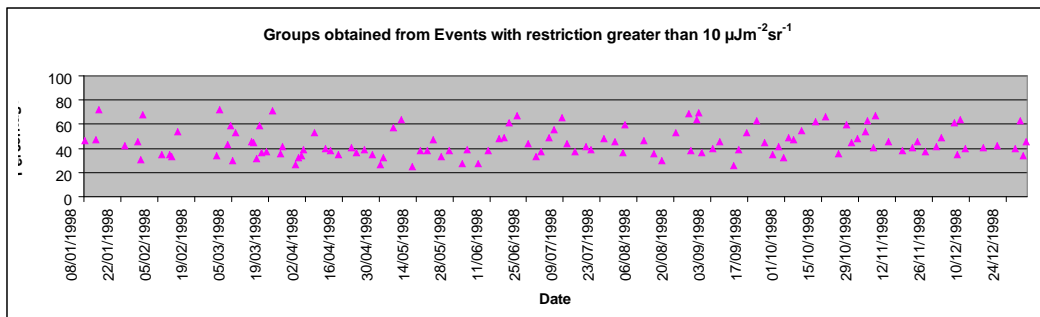


Fig. 16. Comparison between groups derived from events greater than  $10 \mu\text{Jm}^{-2}\text{sr}^{-1}$  and groups derived from events without restriction in radiance

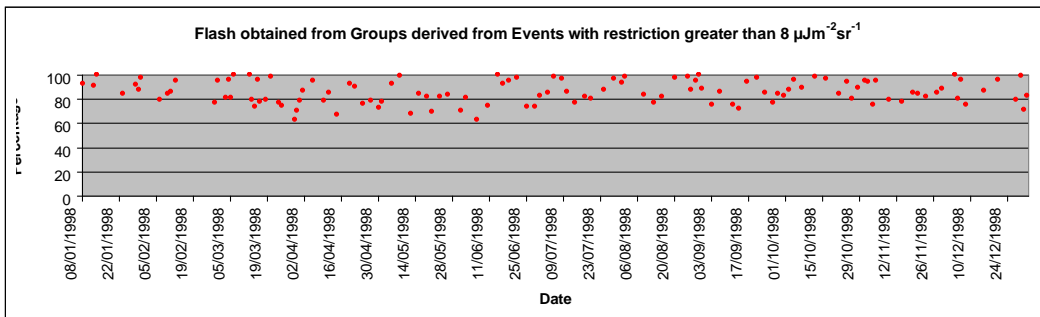


Fig. 17. Comparison between flashes obtained from groups derived from events greater than  $8 \mu\text{Jm}^{-2}\text{sr}^{-1}$ , and the ones with no restriction in radiance

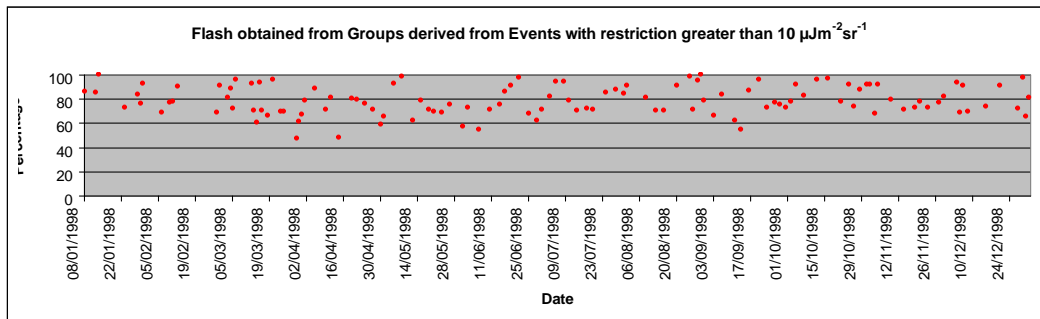


Fig. 18. Comparison between flashes obtained from groups derived from events greater than  $10 \mu\text{Jm}^2\text{sr}^{-1}$ , and the ones with no restriction in radiance

Note, from numbers in Table 4 and graphs in Figure 17 and 18, that the survival percentage of flashes, the most important in this type of phenomenology, stay between 78% and 85%. This first result show the feasibility and the returning value from the use of this instrument (Lightning Imager). Subsequently, was constructed a graph that show the mean survival percentage with standard deviation of events and flashes with distinction in Day, Night and Twilight from analyzed dataset (Figure 19), for the case of radiance greater than  $8 \mu\text{Jm}^2\text{sr}^{-1}$ .

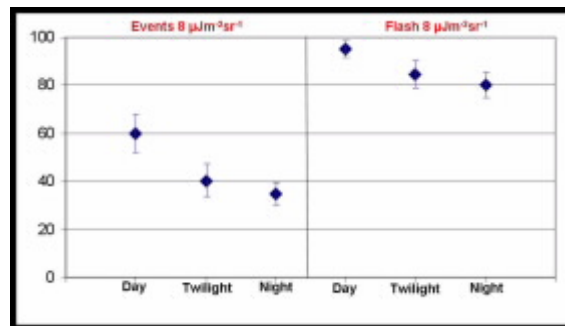


Fig. 19. Mean survival percentage for Events and Flashes greater than  $8 \mu\text{Jm}^2\text{sr}^{-1}$  in Day-Night-Twilight

From events to flashes there is an increase of the mean survival percentage of survivability (around 40%); this demonstrate that the flash assembling technique has capacity for enough flashes reconstruction from initial depleted dataset. This prove that the requirements adopted for the instrument and the utilized technique were well evaluated.

### 3.3 Classes distinction of simulation results.

In the next phase of these analysis we turned our attention to class formation for every processing types (events, groups and flashes). In particular the classes were five, dividing the population of case studies into classes accordingly the percentage of surviving of processing type analyzed, events, groups and flashes with restriction to radiance greater than  $8 \mu\text{Jm}^2\text{sr}^{-1}$  and greater than  $10 \mu\text{Jm}^2\text{sr}^{-1}$ :

- Class 1: 0-20 %
- Class 2: 20-40 %
- Class 3: 40-60 %
- Class 4: 60-80 %
- Class 5: 80-100 %

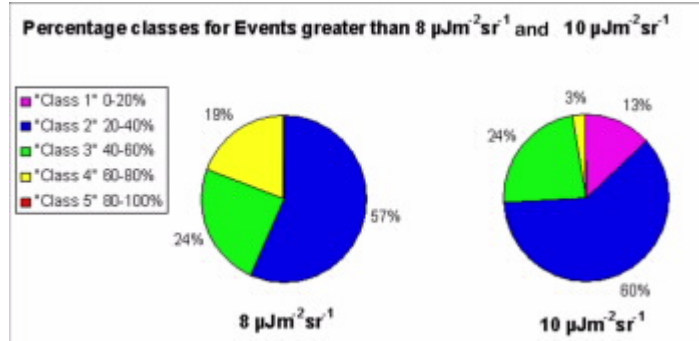


Fig. 20. Percentage classes of case studies events simulated with restriction in radiance greater of 8 and 10  $\mu\text{Jm}^2\text{sr}^{-1}$

Note in Figure 20, the second class is the most important with a percentage from 57 to 60 % of the case studies events belonging to a survival percentage of 20-40 %. The class 3 is the second most important class with a percentage of 24 % of the events belonging to a survival percentage of 40-60 %.

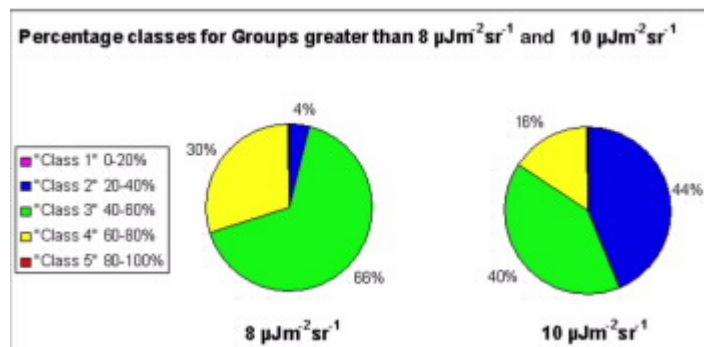


Fig. 21. Percentage classes of case studies groups computed with restriction in events radiance greater of 8 and  $\mu\text{Jm}^2\text{sr}^{-1}$

In Figure 21 the most important classes is the third with a percentage that varies from 40 to 66 % of case studies that correspond to groups in the range of 40-60 % of survivability. The other important classes are the second and the fourth. Note that in this first passage, from events to groups, there is an increase of the percentage of survivability (class number) and this demonstrate the technique ability to save groups during events grouping.

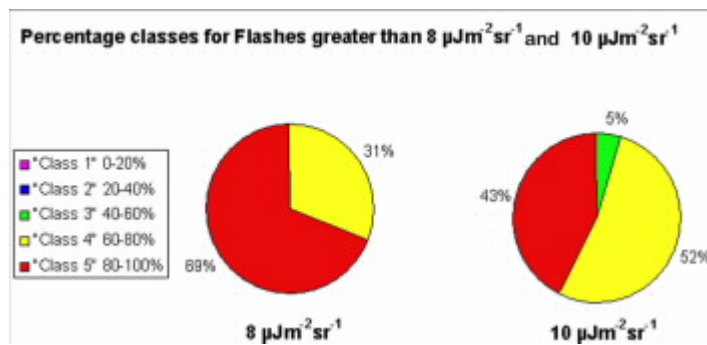


Fig. 22. Percentage classes of case studies flashes computed with restriction in events radiance greater of 8 and  $10 \mu\text{Jm}^2\text{sr}^{-1}$

The latest graph, Figure 22, shows that most populated classes for flashes' detectability are the fourth and the fifth with a percentage of 69 % (at  $8 \mu\text{Jm}^2\text{sr}^{-1}$ ) and of 43 % (at  $10 \mu\text{Jm}^2\text{sr}^{-1}$ ) of simulations with a survivability from 80 to 100 %. This demonstrate finally the technique ability and robustness in observing flashes despite depleted population of survived events.

## 4. CONCLUSIONS

The Centro Nazionale di Meteorologia e Climatologia Aeronautica hosted a fellowship sponsored by Galileo Avionica, for the simulation of MTG-LI sensor behaviour through TRMM-LIS data. We took the expected LI design from MTG Mission Requirement Document, and reprocess real lightning dataset, acquired from space by TRMM-LIS instrument, to produce a simulated MTG-LI lightning dataset. The simulation is performed in several run, varying Minimum Detectable Energy, taking into account processing steps from event detection to final lightning information. A definition of the specific meteorological requirements is given from the potential use in meteorology of lightning final information for convection estimation and numerical cloud modelling. Study results show the range of instrument requirements relaxation which lead to minimal reduction in the final lightning information.

Results show that Lightning Imager instrument, according to the proposed design, relaxing requirements according Option 2.1 of the Meteosat Third Generation Pre-Phase A System Architecture Study-FINAL REPORT, could observe a mean of 85 % of the flashes recorded from a low earth orbit platform, such as TRMM-LIS. These potential observations satisfy the requirements of detecting and monitoring continuously electrical activity "per se" and as a proxy of convection and related phenomena, over global area (full earth disc) resolving the small scale phenomena (meso scale). With Lightning Imager, in fact, it is possible to observe total lightning, cloud-to-cloud and cloud-to-ground discharges, also of weak intensity, while with ground based lightning network, it is possible to observe nearly only cloud-to-ground discharges with high intensity (greater than various kA), a total number of discharges one order of magnitude lower than total lightning. In conclusion, the 85 % of all flashes observed by LI permits an adequate monitoring of all type of phenomenology connected to stormy weather as convection, heavy rain and hail, gusty wind and turbulence.

## REFERENCES

- [1] [http://www.eumetsat.int/home/Main/What\\_We\\_Do/Satellites/Future\\_Satellites/Meteosat\\_Third\\_Generation/index.htm](http://www.eumetsat.int/home/Main/What_We_Do/Satellites/Future_Satellites/Meteosat_Third_Generation/index.htm)
- [2] <http://thunder.nsstc.nasa.gov/>
- [3] Hugh J. Christian, Richard J. Blakeslee, Steven J. Goodman, Douglas A. Mach, Michael F. Stewart, Dennis E. Buechler, William J. Koshak, John M. Hall, William L. Boeck, Kevin T. Driscoll, and Dennis J. Boccippio, THE LIGHTNING IMAGING SENSOR, 1999. [http://thunder.msfc.nasa.gov/bookshelf/pubs/LIS\\_ICAE99\\_Print.pdf](http://thunder.msfc.nasa.gov/bookshelf/pubs/LIS_ICAE99_Print.pdf)
- [4] MTG Team at Alcatel Alenia Space France, Meteosat Third Generation Pre-Phase A System Architecture Study-FINAL REPORT, 2007.
- [5] Hugh J. Christian, Richard J. Blakeslee, Steven J. Goodman, Douglas M. Mach, Algorithm Theoretical Basis Document (ATDB) For The Lightning Imaging Sensor (LIS), 2000.